Pseudoscalar electromagnetic vertex function: Quark-hadron duality

A. N. Kamal and Lo Chong-Huah
Department of Physics, Theoretical Physics Institute, University of Alberta, Edmonton, Alberta, Canada T6G 2J1
(Received 25 March 1985)

A double-dispersion-relation model for the neutral-pseudoscalar-meson—two-photon vertex function is proposed. Several spectral-function sum rules are derived. Quark-hadron duality is established in the model, so that the low-energy behavior of the vertex function is dominated by vector-meson resonances, and the high-energy behavior of the vertex function is determined by QCD dynamics and light-cone algebra. The vertex function is then applied to study the decay processes $\pi^0(\eta^0)\to\gamma\gamma$, $\pi^0(\eta^0)\to e^+e^-(\mu^+\mu^-)$, $\pi^0(\eta^0)\to e^+e^-(\mu^+\mu^-)\gamma$, and the scattering process $e^+e^-\to\pi^0(\eta^0)\gamma$.

I. INTRODUCTION

The pseudoscalar-to-two-photon vertex has been the subject of both experimental and theoretical investigation for several years.[1–9] The off-shell behavior of the vertex effects a variety of processes which can be used as probes. Some of these processes are $\pi^0(\eta^0)\to e^+e^-(\mu^+\mu^-)$, Dalitz-pair decay $\pi^0(\eta^0)\to e^+e^-(\mu^+\mu^-)\gamma$, $e^+e^-\to\pi^0(\eta^0)\gamma$, $e^-e^-\to e^-e^-\pi^0(\eta^0)$, etc.

In $\pi^0(\eta^0)\to e^+e^-(\mu^+\mu^-)$ the vertex function $F_P(k^2;(k-k_P)^2)$ is probed only in an integrated sense as one needs to integrate over all the unphysical photon momenta. In the Dalitz-pair decays one probes the structure of the vertex function at low energies where one would expect the structure to be dominated by vector-meson resonances. On the other hand, in colliding-beam experiments one could probe the structure at very large (~ 10 GeV) incident invariant mass.

There is a quark-hadron duality at work in the following sense. At low energies we expect, from analyticity, that the structure of the vertex will be vector-meson (hadron) dominated. On the other hand, at large values of k^2, for extremely unphysical photons, perturbative QCD (Ref. 10) and light-cone algebra[11] dictate that $F_P(k^2;(k-k_P)^2)$ behave like $1/k^2$. Thus the high-energy behavior is dictated by the quark-gluon dynamics. A model that satisfies both the low-energy and high-energy behaviors alluded to above will be said to satisfy quark-hadron duality.

To the best of our knowledge, two models for $F_P(k^2;(k-k_P)^2)$ have been suggested which satisfy the quark-hadron duality as referred to here. One was suggested by Ma and Babu:[6]

$$F_P(s_1,s_2)=\left[1-\frac{s_1s_2}{3/2m_V{}^2(s_1+s_2-m_P{}^2)}\right]\times\frac{1}{(1-s_1/m_V{}^2)(1-s_2/m_V{}^2)}\ . \tag{1}$$

The other is a simple pole model:[2]

$$F_P(s_1,s_2)=\frac{\Lambda^2}{\Lambda^2-s_1-s_2}\ . \tag{2}$$

It was shown by Bergstrom[5] that the form in (2) can be derived from a potential model for heavy-quarkonium systems. It is unlikely that the same technique would apply to light systems. In any case, (1) and (2) can be treated as phenomenological models for $F_P(s_1,s_2)$.

The quark-hadron duality in the heavy-quarkonium radiative decays has been studied through QCD sum rules.[12] Such a duality has been claimed to be justified in the π^0 electromagnetic decay also since the massive-quark-loop model and the vector-dominance model yield the same slope parameter in $\pi^0\to e^+e^-\gamma$ (Ref. 8).

In this paper, we propose a model for the vertex function which invokes quark-hadron duality in the sense we have described. We postulate that at low energies the vertex is vector-meson (hadron) dominated while at high energies it is constrained by perturbative QCD and light-cone algebra. We write a double dispersion relation for $F_P(s_1,s_2)$ for a fixed $\sqrt{s}=\sqrt{s_1}+\sqrt{s_2}$ in the center of mass. Such a dispersion relation involving a single and a double spectral function is obtained by dispersing in both s_1 and s_2. We constrain the asymptotic properties of $F_P(s_1,s_2)$ through perturbative QCD and light-cone algebra. This leads us to certain spectral-function sum rules which we exploit.

Our estimates of the low-energy processes such as $\pi^0\to\gamma\gamma$, $\eta^0\to\gamma\gamma$, $\pi^0(\eta^0)\to e^+e^-(\mu^+\mu^-)$ and the slope parameter in $\pi^0(\eta^0)\to e^+e^-(\mu^+\mu^-)\gamma$ are not much different from those obtained by vector-meson dominance, which is to be expected. However, our model does give significantly different results from those obtained from traditional vector dominance for high-energy processes such as $e^+e^-\to\pi^0(\eta^0)\gamma$.

This paper is organized as follows. Section II discusses the analytic properties of $F_P(s_1,s_2)$. Asymptotic conditions are imposed on $F_P(s_1,s_2)$ and spectral-function sum rules derived. The parameters of the model are determined and $\pi^0(\eta^0)\to\gamma\gamma$ calculated. In Sec. III, the slope parameter in the Dalitz-pair decays $\pi^0(\eta^0)\to e^+e^-(\mu^+\mu^-)\gamma$ are calculated, as are also the leptonic rates $\pi^0(\eta^0)\to e^+e^-(\mu^+\mu^-)$. In Sec. IV we calculate the cross section for $e^+e^-\to\pi^0(\eta^0)\gamma$. Conclusions follow in Sec. V.

II. THE VERTEX FUNCTION $F_P(s_1,s_2)$

The $P\to\gamma^*(k_1)+\gamma^*(k_2)$ vertex function is defined through

$$\int d^4x\, e^{ik_1\cdot x}\theta(x^0)\langle 0\,|\,[j_\mu^{\rm EM}(x),j_\nu^{\rm EM}(0)]\,|\,P(k_1+k_2)\rangle = i\epsilon_{\mu\nu\alpha\beta}k_1^\alpha k_2^\beta\frac{F_P(k_1^2;k_2^2)}{(2\pi)^{3/2}}\ . \quad (3)$$

The vertex function $F_P(k_1^2,k_2^2)$ satisfies a sidewide-dispersion-relation representation[13] for a fixed value of one of the invariants,

$$F_P(k_1^2;k_2^2)=f_P(k_2)+\frac{1}{\pi}\int\frac{{\rm Im}F_P(s,k_2^2)}{s-k_1^2}ds\ . \quad (4)$$

If both $f_P(k_2)$ and ${\rm Im}F_P(s,k_2^2)$ are real analytic functions of k_2^2, one can disperse in the second variable and write a double dispersion relation for $F_P(k_1^2;k_2^2)$

$$F_P(k_1^2;k_2^2)=\frac{1}{\pi}\int\sigma(s)\left[\frac{1}{s-k_1^2}+\frac{1}{s-k_2^2}\right]ds +\frac{1}{\pi^2}\int\int\rho(s,t)\left[\frac{1}{(s-k_1^2)(t-k_2^2)}\right]\times ds\,dt\ , \quad (5)$$

where $\sigma(s)$ and $\rho(s,t)$ are the single and double spectral functions, respectively, and $\rho(s,t)$ is symmetric in s and t.

In the following, we discuss some constraints on the spectral functions. If one of the two photons is physical, the large-k_1^2 behavior of $F_P(k_1^2;0)$ is predicted by perturbative QCD to be[10]

$$F_{\pi^0}(k_1^2;0)=-\frac{\sqrt{2}f_\pi}{k_1^2}\ ,$$

$$F_\eta(k_1^2;0)=-\frac{\sqrt{2}}{\sqrt{3}}\frac{f_\pi}{k_1^2}\ ,$$

and

$$F_{\eta'}(k_1^2;0)=-\frac{4}{\sqrt{3}}\frac{f_\pi}{k_1^2}\quad (f_\pi\approx 134\ {\rm MeV})\ , \quad (6)$$

which, using (5), leads to two sum rules

$$\int\frac{\sigma_P(s)}{s}ds=0\quad (P=\pi^0,\eta^0) \quad (7)$$

and

$$\frac{1}{\pi}\int\sigma_P(s)ds+\frac{1}{\pi^2}\int\frac{\rho_P(s,t)}{t}ds\,dt=\alpha_P f_\pi\ ,$$
$$\alpha_\pi=\sqrt{2},\quad \alpha_\eta=\sqrt{2}/\sqrt{3},\quad \alpha_{\eta'}=4/\sqrt{3}\ . \quad (8)$$

When both k_1^2 and k_2^2 are in the deep timelike region, the leading term of the asymptotic expansion of the amplitude in (3) is determined by the equal-time commutator of currents[11]

$$\int d^4x\, e^{ik_1\cdot x}\theta(x^0)\langle 0\,|\,[j_\mu^{\rm EM}(x),j_\nu^{\rm EM}(0)]\,|\,P(k_1+k_2)\rangle_{k_1^2\to+\infty} =\frac{i}{k_1^0}\int d^3x\, e^{-ik_1\cdot x}\langle 0\,|\,[j_\mu^{\rm EM}(\mathbf{x},0),j_\nu^{\rm EM}(0)]\,|\,P(k_1+k_2)\rangle+O(1/k_1^2)\ . \quad (9)$$

On the other hand, if both k_1^2 and k_2^2 are in the deep spacelike region, then the behavior of the current commutator in the light-cone region ($x^2\simeq 0$) dominates the transition amplitude in (3). It is believed[14] that the light-cone behavior of hadron current commutators can be determined by the free-quark current. The commutator of electromagnetic currents in the region near the light cone is then obtained as

$$[j_\mu^{\rm EM}(x),j_\nu^{\rm EM}(0)]_{x^2\simeq 0}=\{g_{\mu\alpha}[\bar q(0)Q^2\gamma_\nu q(x)-\bar q(x)Q^2\gamma_\nu q(0)] +g_{\nu\alpha}[\bar q(0)Q^2\gamma_\mu q(x)-\bar q(x)Q^2\gamma_\mu q(0)]-g_{\nu\mu}[\bar q(0)Q^2\gamma_\alpha q(x)-\bar q(x)Q^2\gamma_\alpha q(0)] +i\epsilon_{\mu\nu\alpha\beta}[\bar q(0)Q^2\gamma_5\gamma^\beta q(x)+\bar q(x)Q^2\gamma_5\gamma^\beta q(0)]\}\frac{\partial}{\partial x_\alpha}\Delta(x;m_q^2=0)\ . \quad (10)$$

The operator-product-expansion technique is then applied to the bilocal operator so that

$$\bar q(0)Q^2\gamma_5\gamma^\beta q(x)_{x\to 0} =[1+c(x)+\cdots]\bar q(0)Q^2\gamma_5\gamma^\beta q(0)\ , \quad (11)$$

where $c(x)$ is proportional to the fine-structure constant of QCD and its contribution is suppressed at small x^2 (at large momentum transfer). We ignore the Wilson coefficient $c(x)$ in (11) and define the U(3) vector and axial-vector currents as

$$V_\mu^i(x)=\sum_{a=1}^{3}\bar q_a(x)\frac{\lambda^i}{2}\gamma_\mu q_a(x)\ ,$$

$$A_\mu^i(x)=\sum_{a=1}^{3}\bar q_a(x)\frac{\lambda^i}{2}\gamma_5\gamma_\mu q_a(x)\ ,$$

and

$$V_\mu^{\rm EM}(x)=\sum_{a=1}^{3}\bar{q}_a(x)Q\gamma_\mu q_a(x)\ ,$$

$$Q=\begin{pmatrix}\frac{2}{3} & 0 & 0\\ 0 & -\frac{1}{3} & 0\\ 0 & 0 & -\frac{1}{3}\end{pmatrix}\ . \tag{12}$$

Using the PCAC (partial conservation of axial-vector current) condition

$$\langle 0\,|\,A_\mu^3(0)\,|\,\pi^0(p)\rangle=i\frac{f_\pi}{\sqrt{2}}P_\mu\ ,$$

$$\langle 0\,|\,A_\mu^8(0)\,|\,\eta(p)\rangle=i\frac{f_\pi}{\sqrt{2}}P_\mu\quad (f_{\eta'}=f_\eta=f_\pi)\ , \tag{13}$$

$$\langle 0\,|\,A_\mu^0(0)\,|\,\eta;(p)\rangle=i\frac{f_\pi}{\sqrt{2}}P_\mu\ .$$

We find the large-k^2 (either timelike or spacelike) behavior of $F_P(k^2;(P-k)^2)$ as

$$F_{\pi^0}(k^2;(p-k)^2)_{k^2\to\pm\infty}=-\frac{\sqrt{2}}{3}\frac{f_\pi}{k^2}\ ,$$

$$F_\eta(k^2;(p-k)^2)_{k^2\to\pm\infty}=-\frac{\sqrt{2}}{3\sqrt{3}}\frac{f_\pi}{k^2}\ , \tag{14}$$

and

$$F_{\eta'}(k^2;(p-k)^2)_{k^2\to\pm\infty}=-\frac{4}{3\sqrt{3}}\frac{f_\pi}{k^2}\ .$$

Equation (5) then leads to a sum rule for the single-variable spectral function $\sigma(s)$,

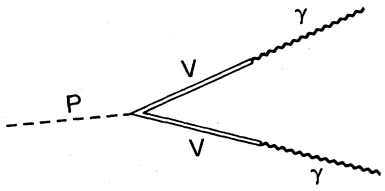

FIG. 1. $P\to\gamma\gamma$ in the vector-dominance model.

$$\frac{1}{\pi}\int\sigma_P(s)ds=\beta_P f_\pi\ ,$$

$$\beta_{\pi^0}=\frac{1}{3\sqrt{2}},\quad \beta_\eta=\frac{1}{3\sqrt{6}},\quad \beta_{\eta'}=\frac{2}{3\sqrt{3}}\ . \tag{15}$$

Substituting (15) into (8), we have the following condition on the double spectral function $\rho_P(s,t)$:

$$\frac{1}{\pi^2}\int\frac{\rho_P(s,t)}{t}ds\,dt=\gamma_P f_\pi\ ,$$

$$\gamma_{\pi^0}=5/3\sqrt{2},\quad \gamma_\eta=5/3\sqrt{6},\quad \gamma_{\eta'}=10/3\sqrt{3}\ . \tag{16}$$

The radiative decay amplitudes of π^0 and η^0 are determined by $\rho(s,t)$ only:

$$F_P(0,0)=\frac{1}{\pi^2}\int\frac{\rho_P(s,t)}{st}ds\,dt\ . \tag{17}$$

The vector-meson-dominance (VMD) model has been used[15] to calculate the two-photon decay processes of neutral pseudoscalar mesons, which are represented by the Feynman diagram in Fig. 1. The strong-interaction vertices in the VMD model are

$$L_S=\Big[-\sqrt{2}g_{VV\phi}\epsilon_{\mu\nu\alpha\beta}(\partial^\mu\omega^\nu)(\partial^\alpha\rho_0^\beta)\pi^0-\frac{g_{VV\phi}}{\sqrt{6}}\epsilon_{\mu\nu\alpha\beta}[(\partial^\mu\rho_0^\nu)(\partial^\alpha\rho_0^\beta)+(\partial^\mu\omega^\nu)(\partial^\alpha\omega^\beta)-2(\partial^\mu\phi^\nu)(\partial^\alpha\phi^\beta)]\eta$$
$$-\frac{g_{VV\phi}}{\sqrt{3}}\epsilon_{\mu\nu\alpha\beta}[(\partial^\mu\rho_0^\nu)(\partial^\alpha\rho_0^\beta)+(\partial^\mu\omega^\nu)(\partial^\alpha\omega^\beta)+(\partial^\mu\phi^\nu)(\partial^\alpha\phi^\beta)]\eta'\Big]\ , \tag{18}$$

where

$$g_{VV\phi}=\frac{3g^2}{16\pi^2 f_\pi}\ ,$$

and the electromagnetic vertices are[15,16]

$$L_{\rm EM}=\sqrt{2}\frac{m_\rho{}^2 e}{g}\left[\rho_0^\lambda+\frac{\omega^\lambda}{3}\right]A_\lambda-\frac{2}{3}\frac{m_\phi{}^2 e}{g}\phi^\lambda A_\lambda\ . \tag{19}$$

(We assume $m_\rho=m_\omega$.)

The predicted radiative decay rates of pseudoscalar neutral mesons are

$$\Gamma(P\to\gamma\gamma)=\frac{\pi\alpha^2}{4}m_P{}^3\,|\,F_P(0,0)\,|^2\ , \tag{20a}$$

where

$$F_{\pi^0}(0,0)=\frac{\sqrt{2}}{4\pi^2 f_\pi},\quad \Gamma(\pi^0\to\gamma\gamma)\simeq 7.6\ \text{eV}\ ,$$
$$F_{\eta^0}(0,0)=\frac{\cos\theta-2\sqrt{2}\sin\theta}{\sqrt{3}}F_{\pi^0}(0,0)\ , \tag{20b}$$
$$\Gamma(\eta^0\to\gamma\gamma)\simeq 0.355\ \text{keV}\ .$$

The physical state η^0 is the linear combination of two isoscalars η and η', i.e.,

$$|\,\eta^0\rangle=\cos\theta\,|\,\eta\rangle-\sin\theta\,|\,\eta'\rangle,\quad \theta\simeq-11.1\ .$$

Our predictions are in agreement with the measured values[17]

$$\Gamma_{\text{expt}}(\pi^0\to\gamma\gamma)=7.9\pm0.55\text{ eV}$$

and (21)

$$\Gamma_{\text{expt}}(\eta^0\to\gamma\gamma)=0.324\pm0.046\text{ keV}\ .$$

Therefore, the double spectral function is dominated by vector-meson poles and has the form

$$\rho_{\pi^0}(s,t)=\frac{\sqrt{2}m_\rho{}^4}{4f_\pi}\delta(s-m_\rho{}^2)\delta(t-m_\rho{}^2)\ ,$$

$$\rho_\eta(s,t)=\frac{5\sqrt{2}m_\rho{}^4}{12\sqrt{3}f_\pi}\delta(s-m_\rho{}^2)\delta(t-m_\rho{}^2)-\frac{\sqrt{2}}{6\sqrt{3}}\frac{m_\phi{}^4}{f_\pi}\delta(s-m_\phi{}^2)\delta(t-m_\phi{}^2)\ ,$$

and (22)

$$\rho_{\eta'}(s,t)=\frac{5m_\rho{}^4}{6\sqrt{3}f_\pi}\delta(s-m_\rho{}^2)\delta(t-m_\rho{}^2)+\frac{m_\phi{}^4}{6\sqrt{3}f_\pi}\delta(s-m_\phi{}^2)\delta(t-m_\phi{}^2)\ .$$

The radiative decay rates do not depend on the value of the vector-meson masses. Using the sum rules in (16), these masses are calculated to be

$$m_\rho=m_\phi=768.5\text{ MeV}\ . \tag{23}$$

The asymptotic chiral symmetry in the spectral function sum rules requires the effective vector-meson mass parameters to be degenerate. Another explanation is that the heavy radially excited vector mesons can effectively shift the mass m_ϕ downward.

The single spectral function plays no role in the radiative decays of pseudoscalar mesons. However, as we shall see in the following sections, when one of the photons is off shell as in Dalitz-pair decay $\pi^0(\eta^0)\to e^+e^-\gamma$, $\pi^0(\eta^0)\to\gamma^*\gamma^*\to e^+e^-(\mu^+\mu^-)$, or $e^+e^-\to\pi^0(\eta^0)$ the single spectral function does play a role.

In the following we construct a phenomenological model for $\sigma(s)$ with a built-in cutoff and constrain its parameters through (7) and (15). We then apply it to $\pi^0(\eta^0)\to e^+e^-(\mu^+\mu^-)\gamma$, $\pi^0(\eta^0)\to\gamma^*\gamma^*\to e^+e^-(\mu^+\mu^-)$, and $e^+e^-\to\pi^0(\eta^0)\gamma$. On general grounds one may postulate the structure of $\sigma(s)$ to be

$$\sigma(s)=G_1\left[\frac{s-4m^2}{s}\right]^{1/2}f_1(s)\theta(s-4m^2)-G_2\left[\frac{s-4M^2}{s}\right]^{1/2}f_2(s)\theta(s-4M^2)\ , \tag{24}$$

where the first term arises from a two-particle intermediate state of particle mass m, while the second term, introduced to secure convergence, is the two-particle state contribution with particle mass M. The square roots are the usual s-wave threshold factors and f_1 and f_2 are some functions of s. G_1 and G_2 are normalizations.

One could have simply used (24) as a phenomenological single spectral function and constrained the parameters by using (7) and (15). We follow a different approach outlined below which builds in the features characterized by (24). In our model $\sigma_{\pi^0}(s)$ is the absorptive part of the Feynman amplitudes shown in Fig. 2.

The four-particle vertices in the diagrams are described by the following effective interaction Lagrangians which have different dimensionalities (higher-dimensional operators are presumably suppressed by large mass scales):

$$\text{(a)}\ L_1=\sum_i g_1^i\epsilon_{\mu\nu\lambda\sigma}F^{\mu\nu}\partial^\lambda\pi^0(\bar{B}_i\gamma^\sigma B_i)\ ,$$

$$\text{(b)}\ L_2=i\sum_i\frac{g_2^i}{m_i}\epsilon_{\mu\nu\lambda\sigma}F^{\mu\nu}\partial^\lambda\pi^0(\bar{B}_i\overleftrightarrow{\partial}{}^\sigma\beta_i)\ , \tag{25}$$

$$\text{(c)}\ L_3=i\left[\sum_i g^i\epsilon_{\mu\nu\lambda\sigma}F^{\mu\nu}(M_i^*\overleftrightarrow{\partial}{}^\lambda M_i)\partial^\sigma\pi^0\right]\ ,$$

where B_i are the charged $J^P=\frac{1}{2}^+$ baryons and their excitations, and M_i are the charged $J^P=0^-$ mesons and their first excitations. In introducing L_1 and L_2 one has to be careful not to disturb the low-energy $\gamma N\to\pi^0 N$ and $\gamma N\to\pi^0\pi N$ phenomenology. Because of the appearance of derivative coupling in L_1 and L_2 the soft-pion theorem,[18] such as the Kroll-Ruderman theorem, are satisfied. The effective Lagrangians L_1 and L_2 can be considered as dispersive corrections to the Born amplitudes of nucleon pole graphs at very low energies. These high-dimension Lagrangians violate unitarity. Their contribution to $E_{1-}(I=0)$, $M_{1+}(I=0)$, and $M_{1-}(I=0)$ in photoproduction vanish at threshold and the correction to $E_{0+}(I=0)$ is small, so that the standard description of low-energy photoproduction through pseudoscalar-vector theory remains undisturbed.

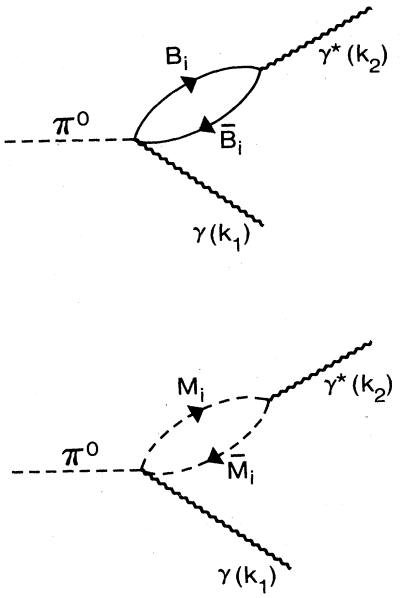

FIG. 2. A model for the single spectral function.

Even though each individual loop in Fig. 2 is quadratically divergent, the contributions of all intermediate states in an SU(3) octet is rendered finite due to the fact that there are equal numbers of positively and negatively charged particles in an SU(3) octet. There are four SU(3) octets in our model; in addition to the ground-state baryon and pseudoscalar-meson octets, the $J^P=\frac{1}{2}^+$ resonances[19] $N^*(1440)$, $\Lambda^*(1600)$, $\Sigma^*(1660)$, and $\Xi^*(1790)$ and $J^P=0^-$ resonances[19] $\pi'(1300)$, $K'(1400)$, and $\eta'(1431)$ are also considered.

If we assume

$$g_m^p=g_m^{\Sigma^+}=g_m^{\Sigma^-}=g_m^{\Xi^-}=g_m,\quad g^\pi=g^K=g\ ,$$
$$g_m^{N^*}=g_m^{\Sigma^{*+}}=g_m^{\Sigma^{*-}}=g_m^{\Xi^{*-}}=g_m^*,\quad g^{\pi'}=g^{K'}=g' \qquad (m=1,2)\ , \tag{26}$$

the cutoff-dependent terms of the Feynman amplitudes, such as Λ^2 and $k^2\ln\Lambda^2$ (for photon off shell), are cancelled. If we impose another condition on the coupling constants,

$$(m_\Xi{}^2-m_p{}^2)g_m=-(m_{\Xi^*}^2-m_{N^*}^2)g_m^*$$
and
$$(m_\pi{}^2-m_K{}^2)g=-(m_{\pi'}{}^2-m_{K'}{}^2)g'\ , \tag{27}$$

then the cutoff-dependent terms $(m_\Xi{}^2-m_p{}^2)g_m\ln\Lambda^2$, $(m_\pi{}^2-m_K{}^2)g\ln\Lambda^2$ are also cancelled. The spectral function $\sigma_{\pi^0}(s)$ is finally

$$\sigma_{\pi^0}(s)=(A_f s+B_f m_p{}^2)(1-4m_p{}^2/s)^{1/2}-(m_p{}^2\leftrightarrow m_\Xi{}^2)+(A_f^* s+B_f^* m_{N^*}{}^2)(1-4m_{N^*}{}^2/s)^{1/2}-(m_{N^*}{}^2\leftrightarrow m_{\Xi^*}{}^2)$$
$$+(A_b s+B_b m_\pi{}^2)(1-4m_\pi{}^2/s)^{1/2}-(m_\pi{}^2\leftrightarrow m_K{}^2)+(A_b' s+B_b' m_{\pi'}{}^2)(1-4m_{\pi'}{}^2/s)^{1/2}-(m_{\pi'}{}^2\leftrightarrow m_{K'}{}^2)\ , \tag{28}$$

where

$$A_f=\frac{1}{6\pi}(g_1+g_2)\ ,$$
$$B_f=\frac{1}{3\pi}(g_1-2g_2)\ , \tag{29a}$$

and

$$A_b=-\frac{g}{24\pi}\ ,$$
$$B_b=\frac{g}{6\pi}\ . \tag{29b}$$

A_f^*,B_f^*,A_b',B_b' can be obtained from A_f,B_f,A_b,B_b by changing g_1,g_2 to g_1',g_2' in (29a) and g to g' in (29b).

Conditions (7) and (15) determine g_1, g_2, and g in terms of f_π. The explicit expressions are given in Eqs. (A1), (A2), and (A3) in the Appendix.

This model predicts the vertex function $F_P(s_1,s_2)$ to be of the form

$$F_{\pi^0}(s_1,s_2)=f(s_1)+f(s_2)+\frac{\sqrt{2}m_\rho{}^4}{4\pi^2 f_\pi}\frac{1}{(s_1-m_\rho{}^2)(s_2-m_\rho{}^2)}\ ,$$
$$F_\eta=\frac{F_{\pi^0}(s_1,s_2)}{\sqrt{3}}\ , \tag{30}$$

and

$$F_{\eta'}=\frac{2\sqrt{2}}{\sqrt{3}}F_{\pi^0}(s_1,s_2)\ ,$$

where

$$f(s)=\frac{1}{\pi}\int\frac{\sigma_{\pi^0}(x)}{x-s}dx\ . \tag{31}$$

The explicit expression of $f(x)$ is given in (A4).

The vector-meson dipole terms dominate the low-energy behavior of the form factor.

III. APPLICATIONS TO DALITZ-PAIR AND LEPTONIC DECAYS

There is a considerable amount of data[20] on Dalitz-pair decays $\pi^0\to e^+e^-\gamma$ and $\eta^0\to\mu^+\mu^-\gamma$, where the vertex functions have been measured as functions of the invariant mass of the Dalitz lepton pair. Even though the integrated rate of the radiative decay $\pi^0\to e^+e^-\gamma$ has already been verified[21] to be insensitive to the π^0-form-factor effect, the structure effects of π^0 can be seen by looking at the rate for events corresponding to significantly large invariant mass of the Dalitz pair. In the kinematic region of Dalitz-pair decays, the vertex function is parametrized by the linear formula

$$F_P(s,0)=F_P(0,0)\left[1+a_P\frac{s}{m_P{}^2}+\cdots\right]\ , \tag{32}$$

where a_P is called the slope parameter. In our model, a_P is the sum of two terms

$$a_P=A_P(V)+A_P(f)\ . \tag{33}$$

The first term $A_P(V)$ is the contribution from the vector-meson pole term. The second term $A_P(f)$ is the contribution from $f(s)$ in Eq. (30). They are given explicitly as

$$A_{\pi^0}(V)=\frac{m_\pi{}^2}{m_\rho{}^2}\ ,$$
$$A_{\eta^0}(V)=\frac{m_\eta{}^2}{m_\rho{}^2}\ ,$$
$$A_{\pi^0}(f)=\frac{m_\pi{}^2}{\pi F_{\pi^0}(0,0)}\int\frac{\sigma(s)}{s^2}ds\ , \tag{34}$$

and

$$A_{\eta^0}(f)=\frac{m_\eta{}^2}{\pi F_{\pi^0}(0,0)}\int\frac{\sigma(s)}{s^2}ds\ .$$

Numerically [we have used m_ρ and m_ϕ from Eq. (23)],

$$A_{\pi^0}(V)=0.033,\quad A_{\eta^0}(V)=0.510\ ,$$
$$\frac{A_{\pi^0}(f)}{A_{\pi^0}(V)}=\frac{A_{\eta^0}(f)}{A_{\eta^0}(V)}=-0.023\ . \tag{35}$$

This result justifies the "vector-meson dominance" in the low-energy region.

The vector-dominance prediction, which remains virtually unchanged by the single spectral function introduced, is in good agreement with the experimental values[22,23]

$$a_{\pi^0}=0.05\pm0.03\ ,$$
$$a_{\eta^0}=0.57\pm0.12\ . \tag{36}$$

The slope parameter of the electromagnetic vertex function has also been estimated in other models. The "traditional" vector-meson-dominance model predicts $a_P=A_P(V)$ with the physical masses of vector mesons. The fermion-loop model[3] gives a simple formula for a_{π^0},

$$a_{\pi^0}=\frac{1}{12}\left[\frac{m_\pi{}^2}{m_f{}^2}\right],$$

which can be consistent with data, if the fermion mass m_f is between 140 and 280 MeV. However, the formulas for a_{η^0} are different in the baryon-loop model[3] and the quark-loop model.[9]

The decay rates of the rare decay processes $\pi^0\to e^+e^-$ and $\eta^0\to\mu^+\mu^-$ depend sensitively on the structure of $\pi^0(\eta^0)\gamma^*\gamma^*$ vertex functions. In an early calculation Drell[1] noted that if the decay goes through a two-photon state and the vertex function $F_P(s_1,s_2)$ is taken to be constant then the real part of the decay amplitude is logarithmically divergent. To the leading order (the fourth order) in electromagnetic interaction and to all orders in strong interaction, the decay amplitude of the $P\to l^+l^-$ mode is

$$M(P\to l^+l^-)=e^4\int\frac{d^4k}{(2\pi)^4}\frac{\epsilon_{\mu\nu\alpha\beta}q^\alpha k^\beta F_P(k^2(k-q)^2)\bar u(p_2)\gamma^\mu(\not k-\not p_1+m_l)\gamma^\nu v(p_1)}{(k^2+i\epsilon)[(k-q)^2+i\epsilon][(k-p_1)^2-m_l{}^2+i\epsilon]}$$
$$=\frac{e^4m_l}{8\pi^2}R_P\bar u(p_2)\gamma_5 v(p_1)\ , \tag{37}$$

which can be represented schematically by the diagram in Fig. 3. The effective coupling constant R_P is related to the vertex function $F_P(k^2;(k-q)^2)$ (Ref. 5),

$$R_P=\frac{i}{\pi^2m_P{}^2}\int\frac{2[q^2k^2-(q\cdot k)^2]F_P(k^2;(k-q)^2)}{(k^2+i\epsilon)[(k-q)^2+i\epsilon][(k-p_1)^2-m_l{}^2+i\epsilon]}d^4k\ . \tag{38}$$

The decay width of this rare decay process is

$$\Gamma(P\to l^+l^-)=\frac{|\mathbf{p}|}{\pi}\alpha^4m_l{}^2[R_e{}^2(R_P)+(\mathrm{Im}R_P)^2]\ . \tag{39}$$

The imaginary part of R_p in the transition amplitude arises from the two-real-photon intermediate state. It gives the unitarity lower bound for the π^0 (η^0) leptonic width,

$$[\Gamma(P\to l^+l^-)]_{\rm unit}=\frac{|\mathbf{p}|}{\pi}\alpha^4m_l{}^2(\mathrm{Im}R_P)^2$$
$$=\frac{\alpha^4m_Pm_l{}^2}{64\pi^3f_\pi{}^2}\left[\frac{F_P(0,0)}{F_{\pi^0}(0,0)}\right]^2$$
$$\times\left[\frac{1}{\beta_P}\left[\ln\frac{1+\beta_P}{1-\beta_P}\right]^2\right],$$
$$\beta_P=(1-4m_l{}^2/m_P{}^2)^{1/2} \tag{40}$$

with numerical values

$$[\Gamma(\pi^0\to e^+e^-)]_{\rm unit}\simeq3.7\times10^{-7}\ \mathrm{eV}\ ,$$
$$[\Gamma(\eta^0\to\mu^+\mu^-)]_{\rm unit}\simeq4.24\times10^{-3}\ \mathrm{eV}\ . \tag{41}$$

We found that the vector-meson pole terms in the vertex function give the dominant contribution to the real part of R_p. To the leading order in m_V/m_P, the dipole form factor predicts[24]

$$B(P\to l^+l^-/2\gamma)_{\rm VMD}=\frac{18\alpha^2}{\pi^2}\frac{m_l{}^2}{m_P{}^2}\left[\ln\frac{m_V}{m_l}\right]^2. \tag{42}$$

In calculating the contribution of $f(s)$ to R_P, we approximated $f(s)$ by a polynomial for $|\sqrt{s}|\leq4$ GeV and by its asymptotic expression $-(f_\pi/3\sqrt{2})(1/s)$ for $|\sqrt{s}|\geq4$ GeV. We found

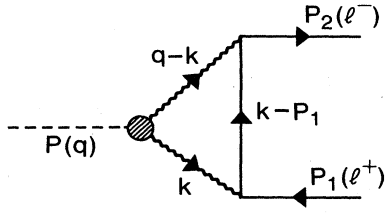

FIG. 3. $P\to l^+l^-$ through 2γ intermediate states.

$$\frac{(R_{\pi^0})_f}{|(R_{\pi^0})_V|}\simeq 0.047$$

and (43)

$$\frac{(R_{\eta^0})_f}{|(R_{\eta^0})_V|}\simeq 0.015 .$$

The predicted decay widths and branching ratios in our model are

$$\Gamma(\pi^0\to e^+e^-)=1.46[\Gamma(\pi^0\to e^+e^-)]_{\text{unit}} ,$$
$$B(\pi^0\to e^+e^-/\gamma\gamma)=0.69\times 10^{-7} ,$$

and (44)

$$\Gamma(\eta^0\to\mu^+\mu^-)=1.31[\Gamma(\eta^0\to\mu^+\mu^-)]_{\text{unit}} ,$$
$$B(\eta^0\to\mu^+\mu^-/\gamma\gamma)=1.40\times 10^{-5} .$$

The prediction for the $\eta^0\to\mu^+\mu^-$ mode is consistent with the recent measurement[25]

$$B(\eta^0\to\mu^+\mu^-/\gamma\gamma)=(1.7\pm 0.7)\times 10^{-5} . \quad (45)$$

However, the predicted branching ratio of the $\pi^0\to e^+e^-$ mode is 3–4 times smaller than the measured value[26]

$$B(\pi^0\to e^+e^-/\gamma\gamma)=(1.8\pm 0.6)\times 10^{-7} . \quad (46)$$

This measured branching ratio of pion leptonic decay requires that the dispersive contribution be about 1.5 times the absorptive contribution. Among the existing models of neutral-pseudoscalar-meson leptonic decays, the recently proposed Tupper-Samuel model[27] gives predictions in good agreement with data. They assume that the decay amplitude is defined by a once-subtracted dispersion relation where the squared mass of pion is the integration variable. Even though a form factor $f(m^2)$ appears at the $(\pi^0)^*\gamma\gamma$ vertex, the two photons are always on the mass shell. The model does not really belong to the type of models which we are studying. Therefore it may not be meaningful to compare their result with ours. It is desirable to measure $\pi^0\to e^+e^-$ again considering that an early measurement of the branching ratio,[28]

$$B(\eta^0\to\mu^+\mu^-/\gamma\gamma)=(5.9\pm 2.2)\times 10^{-5} ,$$

was also much higher than the present value. But if the leptonic width of the pion is really as high as the current experimental value, one may conjecture that the "conventional" theory does not describe the phenomenon. In fact, recently Bergström[5,29] has conjectured that new physics, beyond the standard electroweak theory, may influence the rare decays of π^0. If this is true it would indeed be remarkable that the physics at the scale of 10^2 GeV will be tested at such low energies as the pion mass.

IV. FORM-FACTOR EFFECTS IN $e^+e^-\to\pi^0\gamma,\eta^0\gamma$

The vertex functions $F_P(s,0)$ can also be studied in the $e^+e^-\to\pi^0\gamma$, $\eta^0\gamma$. The low-energy cross section of these processes was calculated in 1970 by Young,[4] who used hard-pion techniques of current algebra to evaluate the matrix elements

$$\langle 0\,|\,\theta(x)[j_\mu^{\text{EM}}(x),j_\nu^{\text{EM}}(0)]\,|\,\pi^0\rangle$$

and

$$\langle 0\,|\,\theta(x_0)[j_\mu^{\text{EM}}(x),j_\nu^{\text{EM}}(0)]\,|\,\eta^0\rangle .$$

High-energy cross sections were later calculated by Dicus, Kolb, and Teplitz,[30] who also estimated the effects of the weak neutral current and the background reaction. They used two models for the $P\gamma^*\gamma^*$ form factors, and found the predictions of these models to be very different. The first model, the pole model of Berman and Geffen,[2] predicts the cross section to go as E^{-4} for high beam energies. The second model, the fermion-loop model,[30] predicts the cross section to go as $(m/2E)^4(\ln 2E/m)^4$, when the beam energy is much higher than the fermion mass m. Owing to the large background reaction rate at high energy, they do not expect to observe the rapid fall-off predicted by the simple pole model.

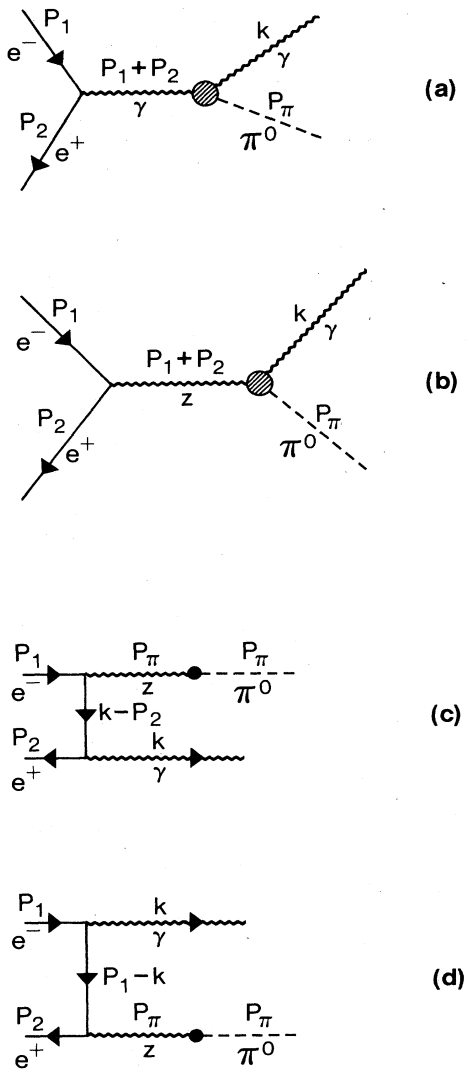

FIG. 4. Diagrams contributing to $e^+e^-\to\pi^0\gamma$.

The transition amplitude for $e^+e^-\to P\gamma$ arises from the processes shown in Fig. 4.

The weak-neutral-current interaction in the standard electroweak theory is given by

$$L_{\rm int}(x)=\left[-\bar{e}\gamma_\mu(g_V+g_A\gamma_5)e(x)+G_V V_\mu^{\rm EM}(x)+G_V' V_\mu^0(x)+G_A\left[A_\mu^3(x)+\frac{A_\mu^8(x)}{\sqrt{3}}-\frac{A_\mu^0(x)}{\sqrt{6}}\right]\right]Z^\mu(x)\ , \tag{47}$$

where the hadronic currents $V_\mu^a(x)$, $A_\mu^a(x)$, and $V_\mu^{\rm EM}$ are defined in (12). The effective couplings are

$$g_V=\frac{g}{\cos\theta_W}\left(\tfrac{1}{4}-\sin^2\theta_W\right),\quad g_A=-\frac{g}{4\cos\theta_W},\quad G_V=\frac{g}{\cos\theta_W}\left(-\tfrac{1}{2}+\sin^2\theta_W\right),\quad G_V'=\frac{g}{2\sqrt{6}\cos\theta_W},\quad G_A=\frac{g}{2\cos\theta_W}\ . \tag{48}$$

Only the vector currents contribute to the $\pi^0\gamma Z$ coupling which can be related to $F_P(s,0)$ by isospin rotation. The matrix element of axial-vector current $\langle 0\,|\,A_\mu^3(x)\,|\,\pi^0,\gamma\rangle$ vanishes by charge-conjugation invariance. The transition amplitude for $e^+e^-\to\pi^0\gamma$ is

$$M(e^+e^-\to\pi^0\gamma)=\epsilon_\mu^*(k)\bar{v}(p_2)\left[\frac{e^3F_\pi^*(s,0)}{s}\epsilon^{\mu\nu\alpha\beta}k_\alpha(p_1+p_2)_\beta\gamma_\nu(A+B\gamma_5)+iC\gamma_5\gamma^\mu+iD^\mu\gamma_5\right]u(p_1)\ , \tag{49}$$

where

$$A=1-\frac{(G_V+\sqrt{3/2}G_V')g_V}{e^2}\frac{s}{(s-M_Z{}^2)},\quad B=-\frac{(G_V+\sqrt{3/2}G_V')g_A}{e^2}\frac{s}{(s-M_Z{}^2)},$$
$$C=-\frac{\sqrt{2}eG_Ag_Af_\pi m_e}{M_Z{}^2}\left[\frac{1}{t-M_Z{}^2}+\frac{1}{u-M_Z{}^2}\right],\quad D^\mu=-\frac{2\sqrt{2}eG_Ag_Af_\pi m_e}{M_Z{}^2}\left[\frac{p_1^\mu}{t-M_Z{}^2}-\frac{p_2^\mu}{u-M_Z{}^2}\right], \tag{50}$$

and

$$s=(p_1+p_2)^2,\quad t=(p_1-k)^2,\quad u=(p_2-k)^2\ .$$

The spin-averaged total cross section of $e^+e^-\to\pi^0\gamma$ is

$$\sigma(e^+e^-\to\pi^0\gamma)=\frac{2\pi^2}{3}\alpha^3\,|F_{\pi^0}(s,0)|^2\frac{(1-m_\pi{}^2/s)^3}{(1-4m_e{}^2/s)^{1/2}}\left[\left[1+\frac{2m_e{}^2}{s}\right]|A|^2+\left[1-\frac{4m_e{}^2}{s}\right]|B|^2\right]$$
$$+\frac{\alpha G_A{}^2g_A{}^2f_\pi{}^2m_e{}^2}{8M_Z{}^4}\left[-\frac{16(m_\pi{}^2/s)}{s(1-4m_e{}^2/s)^{1/2}(1-m_\pi{}^2/s)}+\frac{8(1-m_\pi{}^2/s)}{s(1-4m_e{}^2/s)}\left[1+\frac{2m_\pi{}^2/s}{(1-m_\pi{}^2/s)^2}-\frac{4(m_e{}^2/s)(m_\pi{}^2/s)}{(1-m_\pi{}^2/s)^2}\right]\right.$$
$$\left.\times\ln\left[\frac{1+(1-4m_\pi{}^2/s)^{1/2}}{1-(1-4m_e{}^2/s)^{1/2}}\right]\right]. \tag{51}$$

The transition amplitude and cross section of $e^+e^-\to\eta^0\gamma$ can be obtained from Eqs. (49), (50), and (51) by making the following changes: $F_{\pi^0}\to(s,0)\to F_{\eta^0}(s,0)$, $G_A\to G_A/\sqrt{3}$, and $m_\pi\to m_\eta$.

The first term of Eq. (51), the "direct-channel" contribution, arises from processes shown in Figs. 4(a) and 4(b). The second term, the "crossed-channel" contribution, comes from processes shown in Figs. 4(c) and 4(d). We study the scattering process at beam energies far above the threshold $\sqrt{s}=m_\pi$ but below the Z-boson mass, so that

the final state has a "hard photon" and weak correction is small. Another reason for considering hard photons only is that the bremsstrahlung processes of Figs. 4(c) and 4(d) are expected to be infrared divergent. This divergence is cancelled by virtual photon corrections. To be more specific, the energy region is $3.5 \leq \sqrt{s} \leq 50$ GeV. At $\sqrt{s} = 50$ GeV, the weak correction to the cross section is about 13%. The cross section is predominantly determined by the vertex function $F_P(s,0)$ in this energy region. When the beam energy is sufficiently high (for example, $\sqrt{s} \gtrsim 10$ GeV), $F_{\pi^0}(s,0)$ and $F_{\eta^0}(s,0)$ can be approximated by the expressions

$$F_{\pi^0}(s,0) = f(s) - \frac{\sqrt{2} m_\rho^2}{4\pi^2 f_\pi (s - m_\rho^2)} \approx -\frac{f_\pi/3\sqrt{2}}{s} - \frac{1.18 f_\pi}{s}$$

and

$$F_{\eta^0}(s,0) = \frac{(\cos\theta - 2\sqrt{2}\sin\theta)}{\sqrt{3}} F_{\pi^0}(s,0) \approx \frac{(\cos\theta - 2\sqrt{2}\sin\theta)}{\sqrt{3}} \times \left[-\frac{f_\pi/3\sqrt{2}}{s} - \frac{1.18 f_\pi}{s} \right] . \quad (52)$$

About 17% of $F_{\pi^0}(s,0)$ and $F_{\eta^0}(s,0)$ comes from the single dispersion integral $f(s)$. Our prediction of the cross section is 1.45 times the cross section predicted by the vector-meson (dipole) form factor. Both Ma-Babu[6] and Berman-Geffen[2] form factors become a simple pole when one of the photons is on the mass shell. In Fig. 5, we show the cross sections $\sigma(e^+e^- \to \pi^0(\eta^0)\gamma)$ in the lower-energy region $3 \leq \sqrt{s} \leq 5.5$ GeV. At $\sqrt{s} = 2m_{\Xi}^{*} \simeq 3.6$ GeV. The imaginary part of the amplitude $\pi^0 \to \gamma(N^*, \bar{N}^*) \to \gamma, \gamma^*$ is not cancelled by the corresponding amplitude of $\pi^0 \to \gamma(\Xi^*, \bar{\Xi}^*) \to \gamma, \gamma^*$ which vanishes at the threshold, so it significantly enhances the cross section. Even though the enhancement depends critically on the values of parameters (such as m_{Ξ^*}, $m_{K'}$) of the model, we do expect the cross section to have structure in this energy region.

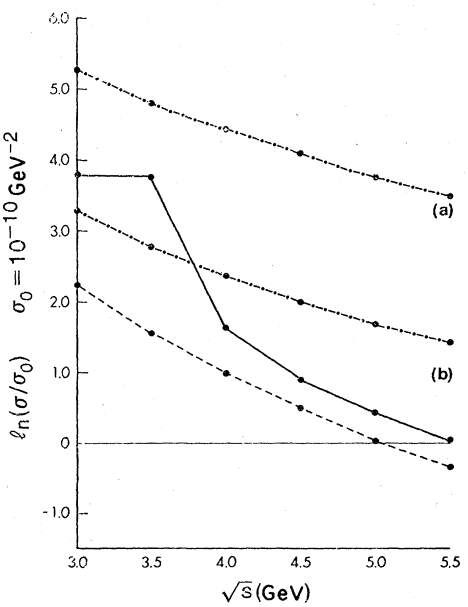

FIG. 5. $\sigma(e^+e^- \to \pi^0\gamma)$ vs $\sqrt{s}$. Dash-dot line, prediction of the fermion-loop model (Ref. 30). Dashed line, prediction of our model with vector pole terms only. Solid line, prediction of our full model. Dash-dot lines (a) and (b) use $m_f = 0.3$ and 0.15 GeV, respectively.

The cross section of the fermion-loop model, with $m_f = 0.15$ and 0.3 GeV, used by Dicus, Kolb, and Teplitz,[30] is also shown in Fig. 5. As one might expect, their cross section does not rapidly fall off with the beam energy. The cross section obtained in the fermion-loop model is also an increasing function of internal fermion mass as the structure is then harder. Since each model makes a very distinct prediction in the intermediate-energy region $3 \lesssim \sqrt{s} \lesssim 5.5$ GeV, experimental data on $e^+e^- \to \pi^0(\eta^0)\gamma$ in this energy region should be valuable to understand the structure of $P\gamma^*\gamma^*$ coupling.

V. CONCLUSION

The structure of the $P\gamma^*\gamma^*$ vertex function $F_P(s_1,s_2)$ can be unravelled by studying $\pi^0(\eta^0) \to \gamma\gamma$, $\pi^0(\eta^0) \to e^+e^-(\mu^+\mu^-)\gamma$, $\pi^0(\eta^0) \to e^+e^-(\mu^+\mu^-)$, $e^+e^- \to \pi^0(\eta^0)\gamma$, and $e^+e^- \to \pi^0(\eta^0)e^+e^-$. Except for the last two processes all the others probe the structure at low invariant mass $\sqrt{s}$ ($\sqrt{s} = \sqrt{s_1} + \sqrt{s_2}$ in the center-of-mass system). In the last two processes the structure may be probed in the region of $\sqrt{s} \sim 10$ GeV.

In this paper, we have proposed a double-dispersion relation for $F_P(s_1,s_2)$ by dispersing in the two invariant masses s_1 and s_2 for a fixed $\sqrt{s}$. We constrain our model by demanding that $F_P(s_1,s_2)$ is resonance dominated at low energies ($s_1,s_2 \sim 1$ GeV^2) and is controlled by quark-gluon dynamics at high energies ($s_1,s_2 \to \infty$). These constraints imply certain spectral-function sum rules which are to fix the parameters of the model.

We conjectured that the double spectral function is vector-meson dominated and used a field theoretical model, only as a device, to parametrize the single spectral function. Only the double spectral function contributes to $\pi^0(\eta^0) \to \gamma\gamma$. The spectral-function sum rules led to effective ϕ-vector-meson masses lower than the measured ones. The lower masses presumably fake the contribution of higher-mass vector mesons which are also expected to contribute.

We found that the effect of the single spectral function on the low-energy processes $\pi^0(\eta^0) \to e^+e^-(\mu^+\mu^-)\gamma$, $\pi^0(\eta^0) \to e^+e^-(\mu^+\mu^-)$ was small. However, its contribution to $e^+e^- \to \pi^0(\eta^0)\gamma$ was quite large. For example, at the invariant energy $\sqrt{s} \gtrsim 10$ GeV the cross section is 45% higher with the single spectral function than without it. Our cross sections for $e^+e^- \to \pi^0\gamma$ as a function of

$\sqrt{s}$ in the region $\sqrt{s} \gtrsim 5$ GeV, are lower than those of Dicus, Kolb, and Teplitz[30] in the fermion-loop model presumably because the form factors are harder in that model. We expect that the single spectral function will be an important contribution to $e^+e^- \to e^+e^-\pi^0(\eta^0)$ also.

ACKNOWLEDGMENT

This work was supported in part by a grant from the Natural Sciences and Engineering Research Council of Canada (NSERC).

APPENDIX

The sum rule in Eq. (7) implies the following relation of the coupling constants g_2 and g in the interaction Lagrangians:

$$g_2=\frac{g}{4}\left[\frac{-m_K^2\ln\frac{m_K^2}{m_\pi^2}+\left[\frac{m_K^2-m_\pi^2}{m_{K'}^2-m_{\pi'}^2}\right]\left[m_{K'}^2\ln\frac{m_{K'}^2}{m_\pi^2}-m_{\pi'}^2\ln\frac{m_{\pi'}^2}{m_\pi^2}\right]}{m_p^2\ln\frac{m_p^2}{m_\pi^2}-m_\Xi^2\ln\frac{m_\Xi^2}{m_\pi^2}+\left[\frac{m_\Xi^2-m_p^2}{m_{\Xi^*}^2-m_{N^*}^2}\right]\left[m_{\Xi^*}^2\ln\frac{m_{\Xi^*}^2}{m_\pi^2}-m_{N^*}^2\ln\frac{m_{N^*}^2}{m_\pi^2}\right]}\right]. \tag{A1}$$

The convergence of the integral in Eq. (15) requires

$$g_1=\frac{g}{4}\left[-\frac{(m_K^2-m_\pi^2)(m_\pi^2+m_K^2-m_{\pi'}^2-m_{K'}^2)}{(m_\Xi^2-m_p^2)(m_p^2+m_\Xi^2-m_{N^*}^2-m_{\Xi^*}^2)}+\frac{-m_K^2\ln\frac{m_K^2}{m_\pi^2}+\left[\frac{m_K^2-m_\pi^2}{m_{K'}^2-m_{\pi'}^2}\right]\left[m_{K'}^2\ln\frac{m_{K'}^2}{m_\pi^2}-m_{\pi'}^2\ln\frac{m_{\pi'}^2}{m_\pi^2}\right]}{m_p^2\ln\frac{m_p^2}{m_\pi^2}-m_\Xi^2\ln\frac{m_\Xi^2}{m_\pi^2}+\left[\frac{m_\Xi^2-m_p^2}{m_{\Xi^*}^2-m_{N^*}^2}\right]\left[m_{\Xi^*}^2\ln\frac{m_{\Xi^*}^2}{m_\pi^2}-m_{N^*}^2\ln\frac{m_{N^*}^2}{m_\pi^2}\right]}\right]. \tag{A2}$$

The sum rule in Eq. (15) also determines g in terms of f_π,

$$\begin{aligned}g^{-1}=\left[\frac{3}{2\sqrt{2}\pi^2 f_\pi}\right]\Bigg\{&-m_K^4\ln\frac{m_K^2}{m_\pi^2}+\left[\frac{m_K^2-m_\pi^2}{m_{K'}^2-m_{\pi'}^2}\right]\left[m_{K'}^4\ln\frac{m_{K'}^2}{m_\pi^2}-m_{\pi'}^4\ln\frac{m_{\pi'}^2}{m_\pi^2}\right]\\&-\frac{(m_K^2-m_\pi^2)(m_{K'}^2+m_{\pi'}^2-m_K^2-m_\pi^2)}{(m_\Xi^2-m_p^2)(m_{\Xi^*}^2+m_{N^*}^2-m_\Xi^2-m_p^2)}\\&\times\left[m_p^4\ln\frac{m_p^2}{m_\pi^2}-m_\Xi^4\ln\frac{m_\Xi^2}{m_\pi^2}+\left[\frac{m_\Xi^2-m_p^2}{m_{\Xi^*}^2-m_{N^*}^2}\right]\left[m_{\Xi^*}^4\ln\frac{m_{\Xi^*}^2}{m_\pi^2}-m_{N^*}^4\ln\frac{m_{N^*}^2}{m_\pi^2}\right]\right]\\&-(m_K^2-m_\pi^2)(m_{K'}^2+m_{\pi'}^2-m_K^2-m_\pi^2)+(m_\Xi^2-m_p^2)(m_{N^*}^2+m_{\Xi^*}^2-m_p^2-m_\Xi^2)\\&\times\frac{-m_K^2\ln\frac{m_K^2}{m_\pi^2}+\left[\frac{m_K^2-m_\pi^2}{m_{K'}^2-m_{\pi'}^2}\right]\left[m_{K'}^2\ln\frac{m_{K'}^2}{m_\pi^2}-m_{\pi'}^2\ln\frac{m_{\pi'}^2}{m_\pi^2}\right]}{m_p^2\ln\frac{m_p^2}{m_\pi^2}-m_\Xi^2\ln\frac{m_\Xi^2}{m_\pi^2}+\left[\frac{m_\Xi^2-m_p^2}{m_{\Xi^*}^2-m_{N^*}^2}\right]\left[m_{\Xi^*}^2\ln\frac{m_{\Xi^*}^2}{m_\pi^2}-m_{N^*}^2\frac{m_{N^*}^2}{m_\pi^2}\right]}\Bigg\}.\end{aligned} \tag{A3}$$

The explicit expression of the single dispersion integral in Eq. (31) is

$$
\begin{aligned}
f(s)=&-\frac{g_2}{\pi^2}\left[\left[m_p{}^2\ln\frac{s}{m_p{}^2}-m_\Xi{}^2\ln\frac{s}{m_\Xi{}^2}\right]-\left[\frac{m_\Xi{}^2-m_p{}^2}{m_{\Xi^*}{}^2-m_{N^*}{}^2}\right]\left[m_{N^*}{}^2\ln\frac{s}{m_{N^*}{}^2}-m_{\Xi^*}{}^2\ln\frac{s}{m_{\Xi^*}{}^2}\right]\right]\\
&+\frac{g}{4\pi^2}\left[m_\pi{}^2\ln\frac{s}{m_\pi{}^2}-m_K{}^2\ln\frac{s}{m_K{}^2}-\left[\frac{m_K{}^2-m_\pi{}^2}{m_{K'}{}^2-m_{\pi'}{}^2}\right]\left[m_{\pi'}{}^2\ln\frac{s}{m_{\pi'}{}^2}-m_{K'}{}^2\ln\frac{s}{m_{K'}{}^2}\right]\right]\\
&+\frac{(g_1+g_2)}{6\pi^2}s\left[\ln\frac{m_\Xi{}^2}{m_p{}^2}-\left[\frac{m_\Xi{}^2-m_p{}^2}{m_{\Xi^*}{}^2-m_{N^*}{}^2}\right]\ln\frac{m_{\Xi^*}{}^2}{m_{N^*}{}^2}\right]-\frac{g}{24\pi^2}s\left[\ln\frac{m_K{}^2}{m_\pi{}^2}-\left[\frac{m_K{}^2-m_\pi{}^2}{m_{K'}{}^2-m_{\pi'}{}^2}\right]\ln\frac{m_{K'}{}^2}{m_{\pi'}{}^2}\right]\\
&+\frac{(g_1+g_2)s+(2g_1-4g_2)m_p{}^2}{6\pi^2}\left[1-\frac{4m_p{}^2}{s}\right]^{1/2}\ln\left[\frac{(1-4m_p{}^2/s)^{1/2}-1}{(1-4m_p{}^2/s)^{1/2}+1}\right]-(m_p{}^2\leftrightarrow m_\Xi{}^2)\\
&-\left[\frac{m_\Xi{}^2-m_p{}^2}{m_{\Xi^*}{}^2-m_{N^*}{}^2}\right]\frac{(g_1+g_2)s+(2g_1-4g_2)m_{N^*}{}^2}{6\pi^2}\left[1-\frac{m_{N^*}{}^2}{s}\right]^{1/2}\ln\left[\frac{(1-4m_{N^*}{}^2/s)^{1/2}-1}{(1-4m_{N^*}{}^2/s)^{1/2}+1}\right]\\
&-(m_{N^*}{}^2\leftrightarrow m_{\Xi^*}{}^2)-\frac{g}{6\pi^2}\left[\frac{s}{4}-m_\pi{}^2\right]\left[1-\frac{4m_\pi{}^2}{s}\right]^{1/2}\ln\left[\frac{(1-4m_\pi{}^2/s)^{1/2}-1}{(1-4m_\pi{}^2/s)^{1/2}+1}\right]+(m_\pi{}^2\leftrightarrow m_K{}^2)\\
&+\frac{g}{6\pi^2}\left[\frac{m_K{}^2-m_\pi{}^2}{m_{K'}{}^2-m_{\pi'}{}^2}\right]\left[\frac{s}{4}-m_{\pi'}{}^2\right]\left[1-\frac{4m_{\pi'}{}^2}{s}\right]^{1/2}\ln\left[\frac{(1-4m_{\pi'}{}^2/s)^{1/2}-1}{(1-4m_{\pi'}{}^2/s)^{1/2}+1}\right]+(m_{\pi'}{}^2\leftrightarrow m_{K'}{}^2)\,. \qquad \text{(A4)}
\end{aligned}
$$

[1]S. D. Drell, Nuovo Cimento **11**, 693 (1959).

[2]S. M. Berman and D. A. Geffen, Nuovo Cimento **18**, 1193 (1960).

[3]M. Pratap and J. Smith, Phys. Rev. D **5**, 2020 (1972).

[4]B. L. Young, Phys. Rev. D **2**, 606 (1970).

[5]L. Bergström, Z. Phys. C **14**, 129 (1982).

[6]K. S. Babu and E. Ma, Phys. Lett. **119B**, 449 (1982).

[7]L. Ametller, L. Bergström, A. Bramon, and E. Masso, Nucl. Phys. **B228**, 301 (1983).

[8]A. Bramon and E. Masso, Phys. Lett. **104B**, 311 (1981).

[9]M. D. Scadron and M. Visinescu, Phys. Rev. D **29**, 911 (1984).

[10]G. P. Lepage and S. J. Brodsky, Phys. Rev. D **22**, 2157 (1980).

[11]J. M. Cornwall, Phys. Rev. Lett. **16**, 1174 (1966); H. Suura, T. F. Walsh, and B. L. Young, Nuovo Cimento **4**, 505 (1972); T. F. Walsh and P. Zerwas, Nucl. Phys. **B41**, 551 (1972).

[12]L. J. Reinders, H. R. Rubinstein, and S. Yazaki, Phys. Lett. **113B**, 411 (1982).

[13]H. Suura and L. M. Simmon, Jr., Phys. Rev. **148**, 1579 (1966); A. M. Bincer, *ibid.* **118**, 855 (1960); S. D. Drell and H. R. Pagels, *ibid.* **140**, B397 (1965).

[14]D. J. Gross and S. B. Treiman, Phys. Rev. D **4**, 1059 (1971); **4**, 210 (1971).

[15]O. Kaymakcalan, S. Rajeev, and J. Schechter, Phys. Rev. D **30**, 594 (1984); M. Gell-Mann, D. Sharp, and W. E. Wagner, Phys. Rev. Lett. **8**, 261 (1962).

[16]N. Kroll, T. D. Lee, and B. Zumino, Phys. Rev. **157**, 1376 (1967).

[17]Particle data group, Rev. Mod. Phys. **56**, S1 (1984).

[18]The review articles on photoproduction of pions are as follows: A. Donnachi, in *High Energy Physics,* edited by E. H. S. Burhop (Academic, New York, 1972), Vol. 6, p. 1; A. Donnachie and G. Shaw, in *Electromagnetic Interactions of Hadrons,* edited by A. Donnachie and G. Shaw (Plenum, New York, 1978), pp. 143–157.

[19]The masses of $(\Xi^-)^*$ and $(\eta')^*$ are calculated by linear and quadratic Gell-Mann–Okubo mass formulas.

[20]J. M. Poutissou, invited paper presented at miniconference on Low Energy Test of Conservation Laws in Particle Physics, Blacksburg, Virginia, 1983 (unpublished).

[21]M. A. Schardt *et al.*, Phys. Rev. D **23**, 639 (1981).

[22]J. Fisher *et al.*, Phys. Lett. **73B**, 359 (1978). The slope parameter a_π is determined to be $a_{\pi 0}=0.10\pm0.03$ (including radiative correction), $a_{\pi 0}=0.05\pm0.03$ (omitting radiative correction).

[23]R. I. Dzhelyadin *et al.*, Phys. Lett. **94B**, 548 (1980).

[24]C. Quigg and J. D. Jackson, Report No. UCRL-18487, 1968 (unpublished).

[25]R. I. Dzhelyadin *et al.*, Phys. Lett. **97B**, 471 (1980).

[26]R. E. Mischke *et al.*, Phys. Rev. Lett. **48**, 1153 (1982).

[27]G. B. Tupper and M. A. Samuel, Phys. Rev. D **26**, 3302 (1982); **29**, 1031 (1983). This model is criticized by L. Bergström and E. Ma, *ibid.* **29**, 1029 (1983).

[28]B. D. Hyams *et al.*, Phys. Lett. **29B**, 128 (1969).

[29]L. Bergström, Phys. Lett. **139B**, 102 (1984).

[30]D. A. Dicus, E. W. Kolb, and V. L. Teplitz, Phys. Rev. D **15**, 1286 (1977).